Diffuse Channel Model and Experimental Results for Array Antennas in Mobile Environments

Ole Nørklit, *Member, IEEE*, and Jørgen Bach Andersen, *Fellow, IEEE*

***Abstract*—A wide-band spatial model of the mobile channel has been developed. The model allows the inclusion of array antennas at the base station. The diffuse scattering is modeled using dense discrete scatterers. An algebraic power decay is used for the pathloss to the scatterers of the environment and to the mobile. Results from the model are compared with experimental results obtained at 1800 MHz. The parameters that are used are delay spread, power window, and angular spread of incident power. The model elucidates the general diffuse background scattering in a rural and an urban environment. It can be extended with inclusion of spatial specular scatterers where appropriate.**

***Index Terms*—Antenna arrays, mobile communication.**

I. Introduction

MODELING the mobile channel has been a subject that has been studied for a long time. Early work studied the received envelope at the mobile and described the behavior statistically by a number of proposed probability density functions (PDF). This work has lead to statistical models such as the Clarke scenario [1], where a number of scatterers are distributed around the mobile at a circle. A wide-band model can be made by using several concentric circles. The scatterers are illuminated by a base station, which is not included in the Clarke model. This rather simple situation shows much of the phenomena that arise in the mobile channel in terms of delay spread and envelope fading and can be used with antenna diversity systems. With the application of antenna arrays at the base station, it is necessary to extend the traditional Clarke model to include the base station. Deterministic approaches such as ray tracing have the advantage of using models of real environments and include both the mobile and the base. This yields an environment with a realistic spread of the signal both in time and angle. On the other hand, statistical models lack the angular information of the environment while concentrating on the signal properties. In this paper, models that have some directional information but also include the generality of the statistical models are developed. It is not the intention to make a deterministic model in which the detailed mechanisms are reflections, diffractions, and scatterings, but to see to what extent these mechanisms collectively can be modeled by a simple effective diffuse model. Previous work with a similar model of diffuse scattering includes [2] where it was shown how propagation parameters influenced the time response with some experimental verification and [3] where probability functions were derived for time and angle for a flat surface. In the present work, a three-dimensional (3-D) approach is taken and experimental results are included. The geometry of the model is based on scattering ellipses, as described in Section II. Section III describes the transfer function of the model where an algebraic power decay is used. Examples of realization of the model are given in Section VI where results obtained from measurements are used to adjust the parameters of the model. Calculation of envelope correlation coefficients is presented at the end of Section VI, followed by a conclusion.

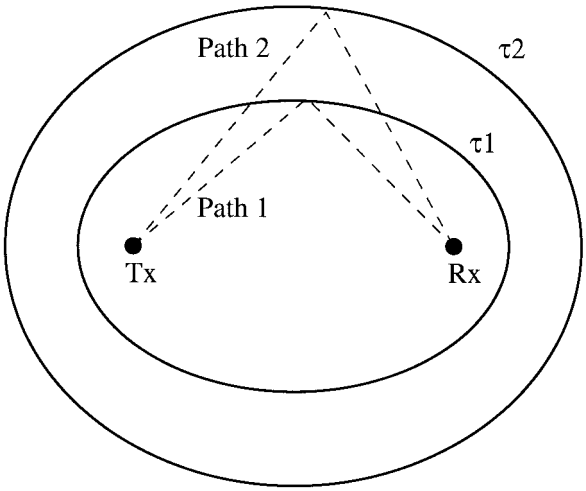

Fig. 1. Transmitter and receiver with scattering ellipses with constant propagation delay.

II. Model Geometry

The basis of the model is the traditional geometry shown in Fig. 1. The transmitter and receiver defines the focal points of ellipses with constant propagation delay. The scatterers are then distributed at these ellipses. This model assumes a single scattering situation (which is often not the case) and multiple scattering will lead to larger delays than given by this model. This model assumes also that the transmitter and receiver has equal antenna heights, which is often the case for indoor systems.

For rural macro cells there is typically a difference of approximately 30 m in antenna heights and for urban micro cells the difference is around 15 m. To be able to include such differences in antenna heights, a 3-D model must be made. This has already been suggested in [4] where scatterers were

Manuscript received February 25, 1997; revised December 29, 1997.

O. Nørklit is with Industrial Research Limited, Lower Hutt, New Zealand.
J. Bach Andersen is with the Center for PersonKommunikation, Aalborg University, Aalborg Denmark.

Publisher Item Identifier S 0018-926X(98)04311-7.

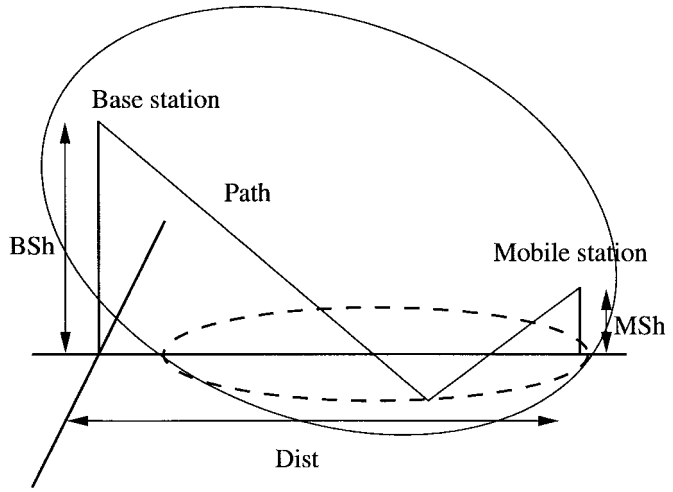

(a)

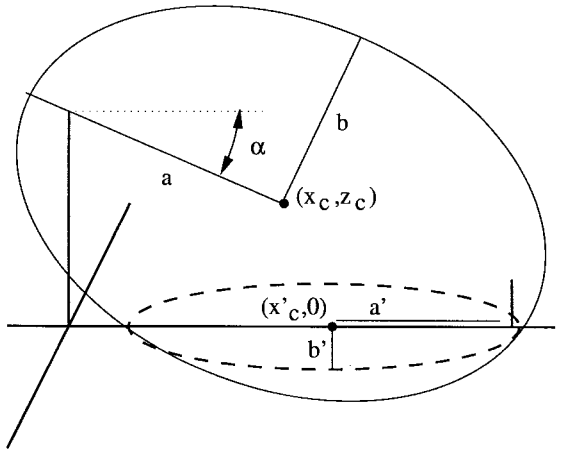

(b)

Fig. 2. Parameters to define ellipsoid and ellipse. (a) Physical parameters. (b) Geometrical parameters.

distributed at cylinders around the mobile to study envelope correlation properties at the base station.

Here, another approach is suggested where the scatterers, in principle, are distributed on ellipsoids. However, to simplify the model, only the intersection of the ellipsoid and the ground is used. This intersection is a new ellipse. The parameters which describe such a scenario are shown in Fig. 2(a), where BSh is the base station height, *MSh* is the mobile station height, *Dist* is the distance between them, and *Path* is the propagation path length, which can be found from the propagation delay τ as $\tau \cdot c$ where c is the propagation velocity. From these parameters, the corresponding ellipsoid that is shown in Fig. 2(b) with major axis $2a$, minor axis $2b$, and tilt angle α can be written as

$$a = \frac{Path}{2} \tag{1}$$

$$b = \sqrt{\frac{Path^2 - (Dist^2 + (BSh - MSh)^2)}{4}} \tag{2}$$

$$\alpha = \tan^{-1}\left(\frac{BSh - MSh}{Dist}\right) \tag{3}$$

From Fig. 2(b), it is also seen that the ellipsoid forms an ellipse at the cut with the ground. In [5], the equation for this ellipse is derived and the result is shown here where $(x'_c, 0)$ is the center of the new ellipse and a' and b' are the new major and minor axes, respectively

$$x'_c = \frac{\left(\frac{1}{b^2} - \frac{1}{a^2}\right) z_c \sin(\alpha)\cos(\alpha)}{\frac{\cos^2(\alpha)}{a^2} + \frac{\sin^2(\alpha)}{b^2}} - x_c \tag{4}$$

$$a' = \sqrt{\frac{1 - \frac{\left(\left(\frac{1}{b^2} - \frac{1}{a^2}\right) z_c \sin(\alpha)\cos(\alpha)\right)^2}{\frac{\cos^2(\alpha)}{a^2} + \frac{\sin^2(\alpha)}{b^2}} - \rho}{\frac{\cos^2(\alpha)}{a^2} + \frac{\sin^2(\alpha)}{b^2}}} \tag{5}$$

$$b' = \sqrt{b^2\left(1 - \frac{\left(\left(\frac{1}{b^2} - \frac{1}{a^2}\right) z_c \sin(\alpha)\cos(\alpha)\right)^2}{\frac{\cos^2(\alpha)}{a^2} + \frac{\sin^2(\alpha)}{b^2}} - \rho\right)} \tag{6}$$

$$\rho = z_c^2\left(\frac{\sin^2(\alpha)}{a^2} + \frac{\cos^2(\alpha)}{b^2}\right). \tag{7}$$

The parameter z_c is the z coordinate or height of the center of the ellipsoid and x_c its the x coordinate. These are given by

$$z_c = \sin(\alpha)\sqrt{a^2 - b^2} + Msh \tag{8}$$

$$x_c = Dist - \cos(\alpha)\sqrt{a^2 - b^2}. \tag{9}$$

With this choice of coordinates, the new ellipse lies in the xy plane. The only parameter that decides the cut is z_c and, therefore, more ellipses can be found at different heights.

A. Scatterer Distribution

In distributing the positions of the scatterers it is assumed that the scatterers are uniformly distributed in the plane and thereby also uniformly distributed at the ellipses lying in the plane. Unlike circles, there exist no simple relation between arclength and angle for ellipses. From the parametric equation for an ellipse $(a'\cos(\Psi), b'\sin(\Psi))$, the following elliptic integral can be derived [5]:

$$s(\Psi) = \int_0^{\Psi} \sqrt{b'^2 + (a'^2 - b'^2)\sin^2(\theta)}\, d\theta. \tag{10}$$

By numerical integration, the circumference $s(2\pi)$ of the ellipse can be found. If the scatterers are distributed uniformly on the interval $[0, s(2\pi)]$, the angles to the scatterers can be found using the same integral in (10). The points in space are then found using this angle and the parametric equation for the ellipse that was used to derive (10). The integral in (10) can also be seen as a distribution function if it is normalized by the circumference. The quantity inside the integral is the probability density function (pdf) of the angles to the scatterers from the center of the ellipse θ_1. As the mobile is placed in a focal point of the ellipse rather than the center, it will be more interesting to know the distribution around the focal point. To find this, the angle, θ_1 must be transformed [5]

$$\theta_2(\theta_1) = \cos^{-1}\left(\frac{\frac{\cos(\theta_1)r + \sqrt{a'^2 - b'^2}}{a'(1-\varepsilon^2)}}{1 + \varepsilon\left(\frac{\cos(\theta_1)r + \sqrt{a'^2 - b'^2}}{a'(1-\varepsilon^2)}\right)}\right) \tag{11}$$

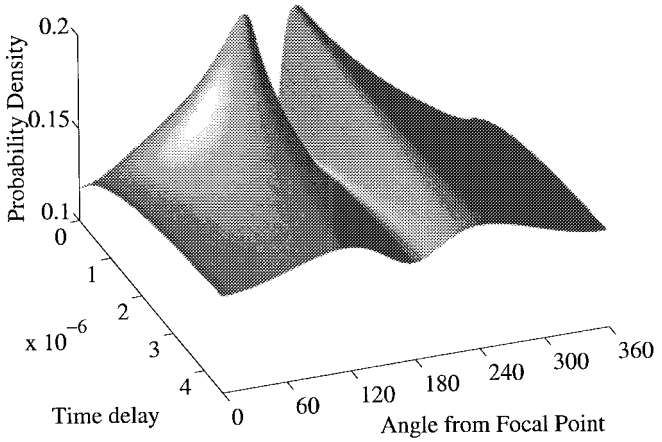

Fig. 3. Probability density of scatterers at different time delays for an urban model as seen from the mobile in one focal point.

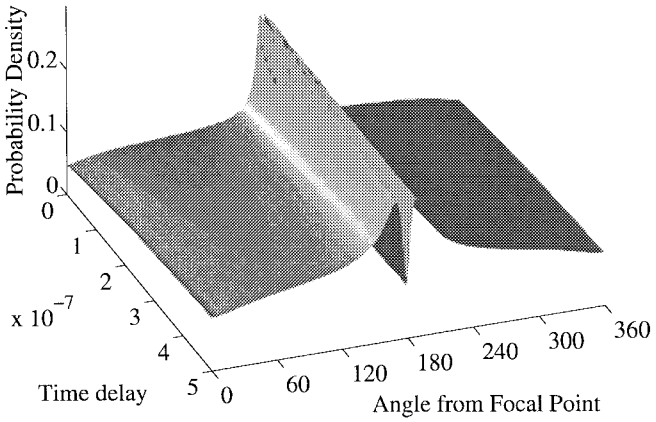

Fig. 4. Probability density of scatterers at different time delays for rural model as seen from the mobile in one focal point.

$$r = \sqrt{\frac{a'^2 b'^2}{a'^2 \sin^2(\theta_1) + b'^2 \cos^2(\theta_1)}} \tag{12}$$

$$\varepsilon = \frac{\sqrt{a'^2 - b'^2}}{a} \tag{13}$$

where θ_2 is the angle from the focal point and θ_1 is the angle from the center. If the transformed angle $\theta_2(\theta_1)$ is substituted into (10) a distribution function for the scatterers around the mobile is obtained when the mobile and base are at the same height

$$f(\theta_2 \mid a', b') = \frac{\sqrt{b'^2 + (a'^2 - b'^2)\sin^2(\theta_2(\theta_1))}}{s(2\pi)}. \tag{14}$$

The axes of the ellipse a' and b' are dependent on the distance between base and mobile and the propagation delay. In Section VI, two models are defined from using measured parameters and the scatterer distributions of these two models are shown in Figs. 3 and 4 as examples. The main thing to observe is that the scatterer distribution around the mobile is not uniform but has two spikes. These arrive from "seeing" down the length of the ellipse. The most dramatic case is the rural model that has a larger distance between base and mobile and a short impulse response making the ellipses long and narrow. For the urban model, the impulse response is longer, yielding more circular-like ellipses and more uniform scatterer distributions.

III. Power Decay versus Distance

From propagation studies, it has been found that the power loss is a power function of distance given as

$$P(x) = \frac{1}{x^\alpha} \tag{15}$$

where α is a constant dependent on the environment. The scattering cross sections for all scatterers are assumed equal. In [2], a similar theory for the time domain was derived. The reason for the increase in pathloss (relative to free-space) is due to the forward scattering of the wave. In Fig. 5 the situation for the mobile case is shown. In Fig. 5, R_m^i is the distance from the mobile to the scatterer i and R_i^0 is the

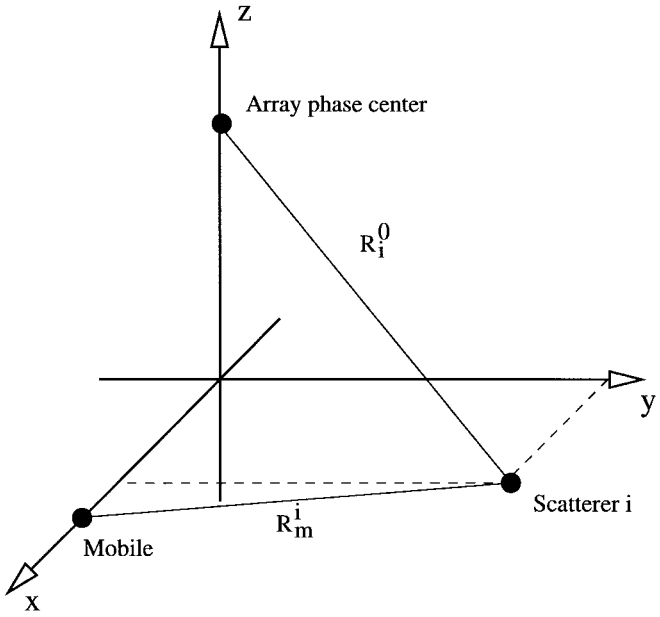

Fig. 5. Definition of path lengths in channel model.

distance from the scatterer i to the array phase center. The pathloss contributions can be written as

$$P(x) = \frac{1}{R_i^0(x)^{\alpha_i}} \cdot \frac{1}{R_m^i(x)^{\alpha_m}} \tag{16}$$

and the two distances are kept apart to make it possible to choose different α for each path, e.g., urban area from the mobile to the scatterer and free-space from scatterer to base. The scatterers near the mobile become more significant than those far from the mobile. To implement the pathloss in the model an amplitude relation is needed, therefore, κ is defined as $\frac{\alpha}{2}$ and an amplitude relation can be written as

$$A(x) = \frac{1}{R_i^0(x)^{\kappa_i}} \cdot \frac{1}{R_m^i(x)^{\kappa_m}}. \tag{17}$$

Using this function the amplitude of the scatterers are weighted by the distances. The frequency domain transfer function for

the nth element of the base station is

$$H(\omega,x,n)=\sum_{i=1}^{S}\underbrace{\frac{1}{R_i^0(x)^{\kappa_i}}\cdot\frac{1}{R_m^i(x)^{\kappa_m}}}_{\text{Distance dependence}}\cdot\underbrace{e^{-jk_b\cdot\left(R_i^0(x)+R_m^i(x)\right)}}_{\text{Phase shift from distance}}\cdot\underbrace{a_ie^{j\theta_i}}_{\text{Scatterer}}\cdot\underbrace{e^{-jt(\vec{k}_m\cdot\vec{v})}}_{\text{Doppler shift}}\cdot\underbrace{e^{-j\vec{k}_b\cdot\vec{x}_n}}_{\text{Array phase}}\cdot\underbrace{D_n(\theta,\phi)}_{\text{Element Pattern}}. \quad (18)$$

The first term is the distance dependence and the second is the phase shift associated with this propagation distance. The reason why the phase constant k has an index b is that the propagation vector has a different direction for mobile to scatterer than for scatterer to base. Of course, the lengths of the two propagation vectors are equal to $\frac{2\pi}{\lambda}$. The term called "scatterer" is the random amplitude and phase of the scatterer. The Doppler shift is dependent on the direction of the propagation vector $\vec{k}_m$ and the velocity vector of the mobile $\vec{v}$. The array is represented by a general equation for arrays where the vector $\vec{x}_n$ is the vector from the phase center to the element n. An element pattern D_n for element n is included, which, in the case of isotropic elements, will be a one.

The basic assumptions of the model are summarized below.

- The waves are plane.
- The model is based upon diffuse scattering with constant scattering cross section.
- Only single scattering occurs.
- There are no specular reflections.
- The time delay between antenna elements can be modeled as phase shifts.

The last assumption is valid as long as the signal has a small relative bandwidth. For applications such as power estimation and direction, finding the frequency-domain model is adequate; but for time-reference adaptive algorithms, a time-domain model must be formulated. Generally, there exist two time dependencies in the model—one associated with the time spread of the signals and one associated with movement of the mobile and thereby the time variance of the model. The time domain model will then be a time-varying impulse response. The phase shift associated with the propagation distance can be written as

$$|\vec{k}_b|\cdot\left(R_i^0(x)+R_m^i(x)\right)=\omega\left(\frac{R_i^0(x)+R_m^i(x)}{c}\right)=\omega\tau_i \quad (19)$$

using that $|\vec{k}_b|=2\pi/\lambda=\omega/c$ where c is the speed of light. The time delay τ_i is associated with the ith scatterer. All scatterers placed on the same ellipse will have same time delay and will, therefore, sum up to be Rayleigh fading. The additional time delay between the antenna elements is modeled as a phase shift. Also, the Doppler shift can be modeled as phase shifts as it arises from the movement of the mobile. With these assumptions, the time-domain channel model can be written as

$$h(\tau,x,n)=\sum_{i=1}^{S}\frac{1}{R_i^0(x)^{\kappa_i}}\cdot\frac{1}{R_m^i(x)^{\kappa_m}}\cdot a_ie^{j\theta_i}\cdot e^{-jt(\vec{k}_m\cdot\vec{v})}\cdot e^{-j\vec{k}_b\cdot\vec{x}_n}\cdot D_n(\theta,\phi)\delta(\tau-\tau_i). \quad (20)$$

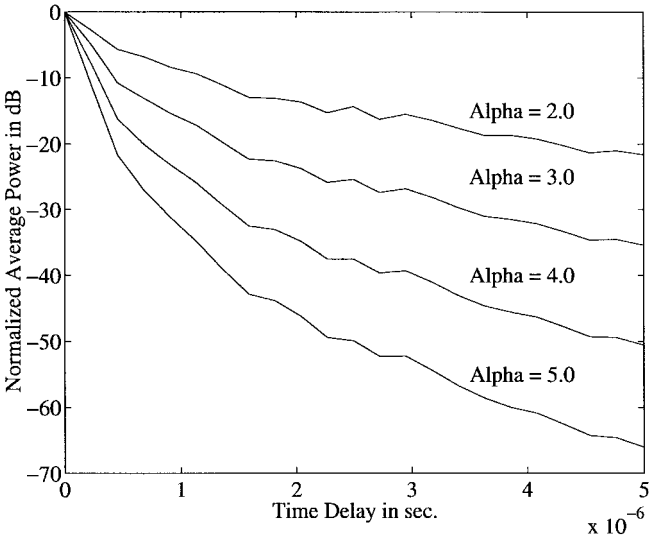

Fig. 6. Average power-delay profiles for varying α.

Examples of average power-delay profiles for different values of α is shown in Fig. 6. The model has a distance between base and mobile of 2 km and a difference in antenna heights of 30 m. The length of the impulse response is 5 μs and the sampling rate is 0.217 μs yielding 23 ellipses. The delay profile and, thus, the delay spread is highly dependent on the α value. In [2], it was shown that the delay spread was infinite for α equal to two. It should be noted that the delay profile for such a diffuse environment is not exponential as is usually assumed. There is a slowly decaying tail, which, in practice, may be drowned in noise.

IV. Scenario Description

A parameter that has become important with the introduction of directional antennas at the base station is the angular spread of the received signal. Here, three methods will be described: the window method and angular spread, which are suggested for scatterer spread estimating in [6]–[8], and horizontal directivity, which is an antenna-related parameter suggested in [9].

The window method is introduced in the characterization of the impulse response in [10]. When the parameters are used to denote angular quantities instead of temporal they are indexed ϕ. A window $W_{\phi q}(x)$ is defined with a length so that the ratio of power inside and outside has the value q here, the denoted in percentage as in [11]. Denoting the received azimuth power pattern as $P(\theta)$

$$q=10\log\left(\frac{\int_{\theta_1}^{\theta_2}P(\theta)\,d\theta}{\int_0^{2\pi}P(\theta)\,d\theta-\int_{\theta_1}^{\theta_2}P(\theta)\,d\theta}\right) \quad (21)$$

$$W_{\phi q}=|\theta_1-\theta_2|. \quad (22)$$

It is chosen to use a power level of 90%, $W_{\phi 90}$.

The angular spread is a statistical description and here the main problem is the circular nature of the received pattern of an antenna, which makes the mean value difficult to define. In [12], the mean value is defined as the direction of the center of mass. The received pattern is then cut 180° from that point to form a linear distribution. This approach is only valid when the power in the cutting zone is low. Also, for nearly omnidirectional distributions, e.g., when the eccentricity of the center of mass is near zero, the mean value loses its meaning. The mean value is then calculated as the direction of the vectorial sum of the pattern vectors

$$\underline{\phi} = \arg \sum \vec{a}. \tag{23}$$

The spread s_ϕ is defined as the standard deviation of the unfolded angular power distribution

$$s_\phi^2 = \oint_\phi \frac{(\phi - \underline{\phi})^2 P(\phi)}{P_{\text{total}}}\, d\phi \tag{24}$$

$$\approx \int_{\phi-180}^{\phi+180} \frac{(\phi - \underline{\phi})^2 P(\phi)}{P_{\text{total}}}\, d\phi \tag{25}$$

where

$$P_{\text{total}} = \int_{\phi-180}^{\phi+180} P(\phi)\, d\phi. \tag{26}$$

The approximation in (25) is only valid for narrow distributions of scatterers. To remove the influence of the antenna used for measuring the angular spread, variance subtraction is used even though the antenna pattern is not a statistical quantity. In [8], it is shown that the variance subtraction not only holds for a convolution, but also for a correlation with the difference of a sign change for the odd moments. The relations are given as [8]

$$s_\phi^2 = s_{M\phi}^2 - s_{A\phi}^2 \tag{27}$$

$$\underline{\phi} = \underline{\phi}_M + \underline{\phi}_A \tag{28}$$

where the subscript M stands for measurement and A for antenna.

For a mechanically rotated antenna, the radiation pattern is constant with direction and thereby the $s_{A\phi}^2$ does not change with the angle. In the case of electronically steered arrays, the shape of the radiation pattern is varying with angle and, therefore, also $s_{A\phi}^2$. If the power is mainly coming from a limited angular spread, the $s_{A\phi}^2$ of the measuring antenna steered to the mean direction can be used as the $s_{A\phi}^2$. For distributions with large spreads, the error introduced will, due to possible broader side lobes, tend to overestimate the spread of the environment.

Another parameter suggested in [13] is the horizontal directivity. This parameter is not statistical, but a two-dimensional form of the normal antenna directivity. The parameter is given as

$$D_{\text{hor}}(\phi_m) = \frac{2\pi \cdot G(\phi_m)}{\sum_{\phi=0}^{2\pi} G(\phi)} \tag{29}$$

where $G(\phi)$ is the horizontal radiation pattern and ϕ_m is the angle of maximum. This parameter describes directional patterns best, but as two different patterns can have the same directivity, the actual shape of the pattern is not described.

For the numerically modeled power-delay profiles in Fig. 6, the delay spread, delay window, scatterer spread, and horizontal directivity has been calculated and is presented in Table I.

TABLE I
ANGULAR AND TIME PARAMETERS FOR SIMULATED PDF

α	s_t [ns]	W_{t90} [ns]	D_{hor} [dB]	s_ϕ
2	907	1950	7.44	15.53°
3	406	434	8.29	12.47°
4	164	217	8.68	11.14°
5	80.6	111	8.82	10.47°

V. MEASUREMENTS

To gain knowledge of the actual scatterer spread in real environments, the scatterer spread has been calculated from (25) using the measurements of the second field trial of RACE project TSUNAMI 1 [12]. As electrical beam steering is going to be used with the channel models, it is also used here for the measurements in order to have comparable results. The data used are the sampled signals at the antenna inputs after an automatic gain control (AGC). The measurements have been performed with eight directive antenna elements in a linear array with $\lambda/2$ spacing. Due to this inherent directionality, the scatterer spread has been calculated in a [−60°; 60°] interval from boresight of the array. From the propagation measurements in [12] with a rotating beam, it has been found that the main part of the received power comes from such an interval around the mean. Two measurement environments have been chosen: an urban site in Kiel, Germany, and a rural site in Aalborg, Denmark.

The results of the calculation of horizontal directivity, angular spread, and angular $W_{\phi 90}$ are given in Table II. The horizontal directivity of the measuring antenna in boresight is 9.4 dB. For the urban case, the spread is varying from 11.2° to 18.1° with a mean of 15.3°. The lowest values are for line-of-sight situations. The $W_{\phi 90}$ does not vary much, but lies around 55°. The horizontal directivity is increasing for decreasing angular spread. When compared to the horizontal directivity of the antenna the environment decreases the directivity by 1–2 dB. For the rural case, the angular spread is ranging from 11.9° to 20.6° with a mean of 14.7°. The horizontal directivity is larger than in the urban case corresponding to the lower angular spread.

When comparing the rural and urban measurements, there is not much difference between the spreading angles. This may be due to the relatively small differences in distances. From the analysis of environments appropriate angular spread of the received signal for two-channel models can be determined, but that is not sufficient as the temporal spread also has to be defined. The delay spread of channel models has been examined before, e.g., in the group special mobile (GSM) standard [14] and in the COST 207 [11] channel profiles have been defined for test of equalizers. These models are used as

TABLE II
ANGULAR PARAMETERS FOR MEASUREMENT ENVIRONMENTS

Scenario	D_{hor} [dB]	s_ϕ	$W_{\phi 90}$	Distance [m]	Line of Sight
Urban1	8.6	13.1°	55.0°	120	Yes
Urban2	8.0	17.8°	51.3°	330→350	No
Urban3	7.1	18.1°	61.9°	70→90	No
Urban4	8.6	11.2°	41.8°	190	Yes
Urban5	7.2	16.5°	54.0°	180→160	Yes→No
Rural1	8.9	14.0°	50.4°	300	Yes
Rural2	8.2	20.6°	64.0°	1200	Yes
Rural3	8.4	15.6°	68.0°	1100	Yes
Rural4	8.8	13.2°	50.6°	1000	Yes
Rural5	8.8	11.9°	49.8°	2000→2500	Yes
Rural6	8.3	13.1°	35.3°	300	Yes

TABLE III
MODEL PARAMETERS FOR SIMULATION MODELS

Type	BSh [m]	MSh [m]	No of tabs	f_c [GHz]	α_m	α_a	Dist. [m]	LoS
Urban	15	2	46	1.8	3.0	2.5	1200	No
Rural	30	2	6	1.8	2.5	2.5	2500	Yes

guidelines for the time dependence of the time/space profiles to be defined in next section. In the COST 207 [11], the delay spread has been defined for a rural area to be within (0.1 $\pm$ 0.02) μs with a delay interval W_{90} of (0.25 $\pm$ 0.15) μs and for a typical urban to be within (1.0 $\pm$ 0.1) μs with a delay interval of (2.3 $\pm$ 0.6) μs in both cases for discrete tabs. In [12], delay spread measurements have been carried out as part of TSUNAMI 1 and here the urban environment has delay spreads ranging from 300 to 600 ns and the rural had at some sites around 40 ns and others around 100 ns. The measurements of field trial from which the angular spread is calculated was performed at the same locations.

VI. MODEL PARAMETERS FROM MEASUREMENTS

With the knowledge given by measurements and previous work, a rural and an urban channel model is defined. As the models are defined by ellipses, the delay spread and angular spread are not independent. It is the time-delay parameter and the distance between base and mobile that determines the shape of the ellipses, which at the same time determines the angular spread. To get both parameters in the right, range compromises have to be made. It is a wish to make the models different so as to be able to test different situations; therefore, it has been chosen to include a line-of-sight for the rural model. The Rice factor is chosen as $k_{\mathrm{Rice}} = 1$ so that the direct signal is equally strong as the sum of scattered signals.

The parameters for the models are given in Table III For the rural case the distance is chosen as the maximum of the measurements. With this distance, it was possible to adjust the model parameters to get time and angular spreads that agreed to those of the measurements.

For the urban case, a distance four to ten times larger than the ones in the measurements is chosen. If shorter distances

TABLE IV
TEMPORAL CHARACTERISTICS FOR SIMULATION MODELS

Type	Delay spread	Delay W_{90}
Urban	782 ns	1590 ns
Rural	147 ns	325 ns

TABLE V
ANGULAR CHARACTERISTICS FOR SIMULATION MODELS

Type	Horizontal Directivity	Angular spread	$W_{\phi 90}$
Urban	8.8 dB	15.8°	58.5°
Rural	11.6 dB	10.1°	33.0°

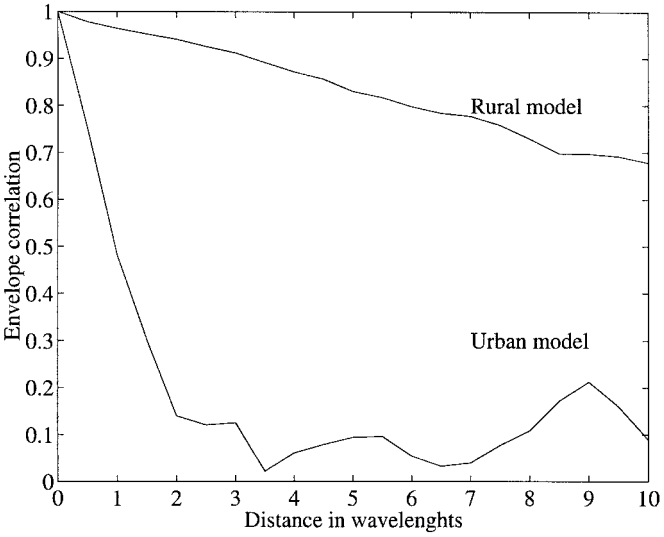

Fig. 7. Envelope correlation for rural and urban models.

are chosen, the angular spread increased for a constant delay spread due to the single scattering property of the model. The reason that measurements show smaller angular spreads for a given delay spread may be caused by multiple scattering.

With the above parameters in the models, the following temporal characteristics have been calculated. In these calculations the mobile is placed in boresight (0°) and the power delay profiles have been averaged over 300 scenarios with different scatterer positions.

As seen in the table, the delay spreads are of the same size as those measured in the TSUNAMI measurements, but for the urban case they are 25% lower than the GSM typical urban (TU) model and for the rural they are 40% higher than GSM rural area.

The angular characteristics are presented in Table V. These are calculated using an 18-element dipole array with a reflector. The antenna has a horizontal directivity of 14.6 dB.

As an example of using the model, the envelope correlation has been calculated at the base station with a 21-element array of dipoles for the two channel models defined in Section VI. The mobile is placed in boresight 0°. The results are shown in Fig. 7. It is seen that the envelope correlation of the rural model decreases slowly and drops under 0.7 at ten wavelengths. For the urban model, the decorrelation is

achieved with much denser spacing, already around one to two wavelengths. The main reason for the difference is the direct path included in the rural model.

VII. Conclusion

A new 3-D ellipsoid model has been used to form an ellipse on which to distribute scatterers. This method takes differences in antenna heights of base and mobile into account. Probability density functions have been derived for the scatterer distribution. Descriptive parameters for angular spread have been discussed and used from measurements to find model parameters. Two channel models have been defined—a rural macro cell model and an urban micro cell model. It is shown that parameters can be chosen such that the characteristics of the model (angular spread and delay spread) are consistent with those for measurements. The envelope correlation has been calculated for the models.

Acknowledgment

The measurements used to gain knowledge of the angular spread were taken during the RACE project TSUNAMI 1. The partners were ERA Technology, Leatherhead, U.K., Alcatel SEL Research Center, Stuttgard, Germany, Hagenuk Gmbh, Kiel, Germany, DETyCom, Spain, Universität Politècnica de Catalunya, Barcelona, Spain, Aalborg University, Aalborg, Denmark, and Bristol University, Bristol, U.K.

References

[1] R. H. Clarke, "A statistical theory of mobile radio reception," *Bell Syst. Tech. J.*, vol. 47, pp. 957–1000, July/Aug. 1969.
[2] J. B. Andersen and P. Eggers, "A heuristic model of power delay profiles in landmobile communications," in *Proc. URSI Int. Symp. Electromagn. Theory*, Sydney, Australia, Aug. 1992, pp. 55–57.
[3] J. C. Liberti and T. S. Rappaport, "A geometrically based model for line-of-sight multipath radio channels," in *46th IEEE Veh. Technol. Conf.*, Atlanta, GA, Apr. 1996, vol. 2, pp. 844–848.
[4] J. D. Parsons and A. M. D. Turkmani, "Characterization of mobile radio signal: Model description," *Proc. Inst. Elect. Eng.*, vol. 138, pt. I, no. 6, pp. 549–556, Dec. 1991.
[5] O. Nørklit, "Adaptive antennas in mobile communication," Ph.D. dissertation, Aalborg University, Aalborg, Denmark, 1996.
[6] P. C. F. Eggers, "Tsunami: Spatial radio spreading as seen by directive antennas," COST 231 TD(95) 119, Darmstad, Germany, Sept. 1995.
[7] P. C. F. Eggers, "Angular dispersive mobile radio environments sensend by highly directive base station antennas," in *Proc. Personal Indoor Mobile Radio Commun.*, Toronto, Canada, Sept. 1995, pp. 522–526.
[8] P. C. F. Eggers, "Quantitative descriptions of radio environments spreading relevant to adaptive arrays," in *Proc. Eur. Personal Mobile Commun. Conf.*, Bologna, Italy, Nov. 1995, pp. 28–30.
[9] O. Nørklit and J. B. Andersen, "Mobile radio environments and adaptive arrays," in *Proc. IEEE Personal Indoor Mobile Radio Commun.*, Hague, Holland, Sept. 1994, pp. 725–728.
[10] J.-P. deWeck and J. Ruprecht, "Real-time ml estimation of very frequency selective multipath channels," in *IEEE Global Telecommun. Conf.*, San Diego, CA, 1990, pp. 2045–2050.
[11] COST207, *Digital Land Mobile Radio Communications*, Commission of the Eur. communities, 1988.
[12] P. Eggers, G. Petersen, and K. Olesen, "Multisenor propagation," deliverable R2108/AUC/WP3./DS/I/046/b1, RACE TSUNAMI.
[13] O. Nørklit, P. Eggers, and J. B. Andersen, "Jitter diversity in multipath envronments," in *IEEE Proc. Veh. Technol. Conf.*, Chicago, IL, July 1995, pp. 853–857.
[14] GSM Recommendations 05.05, *Propagation Conditions.*, ch. annex 3, grp. special mobile, 1988.

Ole Nørklit (S'92–M'96) was born in Denmark in 1968. He received the M.S. degree in electrical engineering from Aalborg University, Denmark, in 1992 and the Ph.D. degree from the Center for PersonKommunikation, Aalborg University, in 1996.

From 1992 to 1993, he was with Aalborg University as a Research Assistant working with spherical near-field antenna measurements. Since December 1996 he has been with Industrial Research Limited, New Zealand, as a Post-Doctoral Fellow. His current interest include mobile communication, channel modeling adaptive antennas, and array signal processing.

Jørgen Bach Andersen (M'68–SM'78–F'92) received the M.Sc. and Doctor of Technology degrees from the Technical University of Denmark (TUD), Lyngby, in 1961 and 1971, respectively.

From 1961 to 1973, he was with the Electromagnetics Institute at TUD and since 1973 he has been with Aalborg University, Denmark, where he is a Professor of radio communications. He has been a Visiting Professor in Tucson, AZ, Christchurch, New Zealand, and Vienna, Austria. Since 1993 he has been head of the Centre for Personkommunikation (CPK), dealing with modern wireless communications. He has been widely published in the areas of antennas, radio-wave propagation, and communications and has also an interest in the biological effects of electromagnetic systems.

Dr. Bach Andersen is a former Vice President of URSI. He is on the Management Committee for COST 259 (a collaborative European program on mobile communications).